

How optimal allocation of limited testing capacity changes epidemic dynamics

Justin M. Calabrese^{1, *} and Jeffery Demers²

¹Center for Advanced Systems Understanding (CASUS), Goerlitz, Germany

²Dept. of Biology, University of Maryland, College Park, MD, USA

*Corresponding author; Email: j.calabrese@hzdr.de

Abstract

Insufficient testing capacity continues to be a critical bottleneck in the worldwide fight against COVID-19. Optimizing the deployment of limited testing resources has therefore emerged as a keystone problem in pandemic response planning. Here, we use a modified SEIR model to optimize testing strategies under a constraint of limited testing capacity. We define pre-symptomatic, asymptomatic, and symptomatic infected classes, and assume that positively tested individuals are immediately moved into quarantine. We further define two types of testing. Clinical testing focuses only on the symptomatic class. Non-clinical testing detects pre- and asymptomatic individuals from the general population, and an “information” parameter governs the degree to which such testing can be focused on high infection risk individuals. We then solve for the optimal mix of clinical and non-clinical testing as a function of both testing capacity and the information parameter. We find that purely clinical testing is optimal at very low testing capacities, supporting early guidance to ration tests for the sickest patients. Additionally, we find that a mix of clinical and non-clinical testing becomes optimal as testing capacity increases. At high but empirically observed testing capacities, a mix of clinical testing and unfocused (information=0) non-clinical testing becomes optimal. We further highlight the advantages of early implementation of testing programs, and of combining optimized testing with contact reduction interventions such as lockdowns, social distancing, and masking.

Keywords: COVID-19; Epidemiology; Optimal control; SARS-CoV-2; SEIR Model

Introduction

The COVID-19 pandemic caught the world off-guard and continues to result in devastating consequences to life, health, and national economies. A key factor hampering global control efforts has been the unanticipated shortage of testing capacity. While testing was clearly problematic early in the pandemic, it remains a critical bottleneck in many parts of the world despite massive efforts to ramp up capacity ([Hasell et al., 2020](#)). Extensive testing provides the empirical basis on which to build a robust, scientifically based response strategy ([Grassly et al., 2020](#)). Insufficient testing leaves public health authorities with little information on how to coordinate efforts to effectively

28 combat an emerging epidemic. For example, [Li et al. \(2020\)](#) estimated that, early in the COVID-
29 19 outbreak in China, 86% of infections went undocumented, and these unnoticed cases fueled
30 the subsequent global expansion of the disease. Similarly, undetected introductions of the virus
31 coupled with undocumented community transmission facilitated the rapid spread of COVID-19 in
32 New York City ([Gonzalez-Reiche et al., 2020](#)). Sustained high-rate testing also plays a crucial
33 role in strategies for safely moving beyond costly and crippling lockdowns ([Grassly et al., 2020](#)).
34 Specifically, quick identification and isolation of new infection clusters is critical for managing a
35 disease like COVID-19 before a vaccine is widely available.

36 While other aspects of epidemic response such as vaccine distribution have been studied from a
37 resource allocation perspective ([Zaric and Brandeau, 2001](#); [Hansen and Day, 2011](#); [Emanuel et al.,](#)
38 [2020](#)), the optimal allocation of limited testing capacity has, so far, received little attention ([Grassly](#)
39 [et al., 2020](#)). The limited work that has been done on this topic has emerged recently, with some
40 efforts focusing on using pooled testing as a simple means to stretch limited testing capacity as far
41 as possible ([Aragón-Caqueo et al., 2020](#); [de Wolff et al., 2020](#); [Ghosh et al., 2020](#); [Gollier and Goss-](#)
42 [ner, 2020](#); [Jonnerby et al., 2020](#)), while others consider stratified testing strategies focused on high
43 risk groups such as health care workers ([Cleevely et al., 2020](#); [Grassly et al., 2020](#)). Mathematical
44 optimization has been applied to the economics of lockdown and quarantine policies ([Aldila et al.,](#)
45 [2020](#); [Alvarez et al., 2020](#); [Choi and Shim, 2021](#); [Jones et al., 2020](#); [Khatua et al., 2020](#); [Piguillem](#)
46 [and Shi, 2020](#)), and to parameter estimation using testing data ([Chatzimanolakis et al., 2020](#)), but
47 has not yet been applied comprehensively to resource allocation problems under testing constraints.

48 Faced with insufficient testing capacity, public health agencies advise the prioritization of test-
49 ing effort via qualitative considerations ([Centers for Disease Control and Prevention, 2020](#)). These
50 guidelines base resource allocation decisions on total testing capacity, quality of information gained
51 via contact tracing, current outbreak stage, and other characteristics specific to individual com-
52 munities ([Centers for Disease Control and Prevention, 2020](#)). The proportion of limited testing
53 resources reserved for high priority cases (e.g., highly symptomatic and vulnerable patients, essen-
54 tial healthcare workers) depends in part on the overall degree of sporadic versus clustered versus
55 community-wide transmission ([Robert Koch Institute, 2020](#); [World Health Organization, 2020b](#)).
56 While these recommendations provide useful qualitative guidance, quantitative determination of
57 optimal allocation strategies under limited testing is lacking despite its potential to increase testing

58 efficiency.

59 Here, we address the optimal allocation of limited testing capacity with a COVID-19 specific
60 SEIR ordinary differential equation compartmental model that features constrained testing and
61 quarantine. We consider the allocation of testing and health care resources between two broad
62 strategies ([Centers for Disease Control and Prevention, 2020](#); [Robert Koch Institute, 2020](#); [World
63 Health Organization, 2020b](#)): 1) clinical testing focused on moderate to severely symptomatic
64 cases, and 2) non-clinical testing designed to detect mildly symptomatic, pre-symptomatic, or fully
65 asymptomatic cases. We further explore how the quality of proxy information with which to focus
66 non-clinical testing on infected individuals affects the optimal balance between strategies. For both
67 strategies, we assume that individuals that test positive are immediately moved into quarantine.
68 We first quantify the extent to which an outbreak can be suppressed via optimal testing and quaran-
69 tine as a function of both testing capacity and proxy information quality. Specifically, we identify
70 strategies that minimize the peak of the infection curve (i.e., “flatten the curve”). We then con-
71 sider how positive factors like social distancing measures, and detrimental factors such as delays in
72 testing onset affect optimal testing strategies and outbreak controllability. Throughout, we focus
73 our analyses on empirically supported parameter values including realistic testing rates. While
74 many existing COVID-19 SIR-like compartmental models explore the effects testing with forms
75 of isolation like quarantine or hospitalization, the majority of these studies assume simple linear
76 equations for the rates at which tests are administered and individuals are isolated ([Adhikari et al.,
77 2021](#); [Ahmed et al., 2021](#); [Amaku et al., 2021](#); [Choi and Shim, 2021](#); [Dwomoh et al., 2021](#); [Hussain
78 et al., 2021](#); [Ngonghala et al., 2020](#); [Rong et al., 2020](#); [Saldaña et al., 2020](#); [Sturniolo et al., 2021](#);
79 [Tuite et al., 2020](#); [Verma et al., 2020](#); [Youssef et al., 2021](#)). We show (see [Methods: Testing model](#))
80 that linear models can not fully describe highly limited testing capacity scenarios, and we pro-
81 pose a novel, non-linear testing model that flexibly accounts for resource-rich and resource-limited
82 settings.

83 **Methods**

84 **Model development**

85 We develop a modified SEIR model to determine how limits on the number of tests administered per
86 day influence disease controllability, and to determine how limited resources can be best distributed
87 among compartments in the modeled population. Our study was motivated by the COVID-19
88 crisis, both in terms of model structure, and in terms of the pressing need to make the most of
89 limited testing capacity. Following other COVID-19 models ([Contreras et al., 2020](#); [Hellewell et al.,
90 2020](#); [Kretzschmar et al., 2020](#); [Liu et al., 2020b](#); [Piasecki et al., 2020](#); [Rong et al., 2020](#)), we
91 assume two separate infectious categories based on observable symptoms. One, the “symptomatic
92 class,” collects moderate to severely symptomatic cases for which one would typically seek clinical
93 treatment, and the other, the “asymptomatic class,” collects all remaining cases, which may be
94 either properly asymptomatic, or may simply be mild enough that the infected individual does
95 not consider themselves sick or seek clinical treatment. We first develop a baseline disease model
96 without interventions, and then incorporate testing and quarantine control strategies.

97 **Baseline SEIR model**

98 We assume a homogeneously mixed population divided into S susceptible, E exposed, A asymp-
99 tomatic and infectious, Y symptomatic and infectious, and R recovered classes. Newly infected
100 individuals first enter the exposed class where they are unable to transmit the disease, and after
101 a latent period, will enter the symptomatic or asymptomatic infectious class. For clarity, we take
102 “asymptomatic” to include individuals who will show only mild to no symptoms over the course
103 of the disease. The portion of individuals in the exposed class who eventually transition to the
104 symptomatic class are considered “pre-symptomatic”. Although some evidence suggests that pre-
105 symptomatic individuals can begin transmitting the disease one to several days before showing
106 symptoms ([Furukawa et al., 2020](#); [He et al., 2020](#); [Walsh et al., 2020](#)), for simplicity, we assume
107 that only A and Y class individuals are infectious. We further assume no host births or deaths,

108 and that recovered hosts obtain permanent immunity. The model equations are as follows:

$$\dot{S}(t) = -\lambda_A \beta \frac{A(t)}{Z} S(t) - \lambda_Y \beta \frac{Y(t)}{Z} S(t) \quad (1a)$$

$$\dot{E}(t) = \lambda_A \beta \frac{A(t)}{Z} S(t) + \lambda_Y \beta \frac{Y(t)}{Z} S(t) - \varepsilon E(t) \quad (1b)$$

$$\dot{A}(t) = f_A \varepsilon E(t) - rA(t) \quad (1c)$$

$$\dot{Y}(t) = f_Y \varepsilon E(t) - rY(t) \quad (1d)$$

$$\dot{R}(t) = rA(t) + rY(t). \quad (1e)$$

109 Here and throughout this paper, over dots denote derivatives with respect to time, and we mea-
110 sure time in units of days. The meaning of each model parameter, and the numerical values used,
111 are given in Table 1. We note that while the recovery time $1/r$ and incubation period $1/\varepsilon$ can be
112 consistently estimated from data, some parameters in our model not accurately known. Specifically,
113 the fractions of asymptomatic and symptomatic infectious populations, f_A and f_Y , respectively, are
114 highly uncertain parameters, as estimates based on both modeling and clinical data place the truly
115 asymptomatic population anywhere from 1% to 80% of all infections ([Furukawa et al., 2020](#); [Walsh](#)
116 [et al., 2020](#); [Widders et al., 2020](#)). Focusing on symptomatic individuals, the fractions that are
117 mildly symptomatic versus moderately to severely symptomatic are also uncertain, although some
118 evidence suggests the majority of cases are mild ([Liu et al., 2020a](#)). Based on these observations,
119 we choose $f_A = 0.75$ and $f_Y = 0.25$ as baseline values. Studies quantifying viral loads via RT-
120 PCR tests and viral culture studies generally show that asymptomatic individuals are as, or less,
121 infectious than symptomatic individuals ([Walsh et al., 2020](#); [Widders et al., 2020](#)), and that more
122 severely symptomatic cases can be associated with higher viral loads ([Liu et al., 2020a](#); [Walsh et al.,](#)
123 [2020](#); [Widders et al., 2020](#)). We therefore assume that the symptomatic transmission probability,
124 λ_Y , is twice that of the asymptomatic transmission probability, λ_A . Finally, we choose the overall
125 values of λ_A , λ_Y , and the contact rate, β , to yield a basic reproduction number of $R_0 = 5.0$ absent
126 of any testing or quarantine control (see the [Appendix](#) for an analytic expression for R_0). This
127 R_0 value falls roughly in the middle of the ranges suggested by a number of studies ([Jiang et al.,](#)
128 [2020](#); [Majumder and Mandl, 2020](#); [Rong et al., 2020](#); [Sanche et al., 2020](#)). Note that under our
129 model parameters, in the absence of testing and quarantine, the symptomatic and asymptomatic

130 contributions to R_0 are 2.0 and 3.0, respectively.

131 **Testing model**

132 To analyze testing and quarantine control strategies operating with testing capacity constraints,
133 we construct a simple model that scales smoothly between extremes of abundant and severely
134 constrained testing resources. This model is governed by the testing capacity, C , and the testing
135 time, τ . The testing capacity C denotes the maximum achievable per capita testing rate assuming a
136 fixed level of resources. This maximum testing rate represents the limitations of a finite health care
137 infrastructure and finite testing supplies, and we take “increased resources” to mean an increased
138 value of C . The testing time represents the average amount of time required for an individual
139 be tested and obtain results, absent any backlogs or waiting times due to other patients. Time-
140 consuming factors independent of the number of people needing to be tested determine the value of
141 τ , for example, procrastination, travel time, and test processing times. Suppose that some sub-
142 population $P(t)$ of the total population Z is eligible to be tested at time t , and let $\dot{T}(t)$ denote the
143 rate at which tests are administered and processed for results. We propose the following expression:

$$\dot{T}(t) = \frac{P(t)}{\tau + \frac{P(t)}{CZ}}. \quad (2)$$

144 Under this model, $\dot{T}(t)$ falls between two limiting expressions representing “resource-limited” and
145 “testing time-limited” testing regimes, defined by $\frac{P(t)/\tau}{CZ} \gg 1$ and $\ll 1$, respectively:

$$\dot{T}(t) = \begin{cases} CZ, & \frac{P(t)/\tau}{CZ} \gg 1 \text{ (resource-limited)} \\ \frac{P(t)}{\tau}, & \frac{P(t)/\tau}{CZ} \ll 1 \text{ (testing time-limited)}. \end{cases} \quad (3)$$

146 The testing time-limited regime represents a high resource availability scenario, where the total
147 testing rate is limited only by the rate at which individuals arrive to be tested and the actual time
148 required for a single test to produce results. The resource-limited regime represents a low resource
149 availability scenario, where the number of people needing to be tested far exceeds the maximum
150 daily testing capacity.

151 It is important to note that despite its frequent use in the literature, a simple linear testing

Parameter	Name	Meaning	Value	Refs
β	Contact rate	Average number of contacts per individual per unit time	4.0*	Jiang et al. (2020); Majumder and Mandl (2020); Rong et al. (2020); Sanche et al. (2020)
λ_A	Asymptomatic transmission probability	Probability of disease transmission per susceptible-symptomatic contact	0.125*	Jiang et al. (2020); Majumder and Mandl (2020); Rong et al. (2020); Sanche et al. (2020)
λ_Y	Symptomatic transmission probability	Probability of disease transmission per susceptible-asymptomatic contact	$2\lambda_A^*$	Liu et al. (2020a); Walsh et al. (2020); Widders et al. (2020)
$1/\varepsilon$	Latent period or incubation period	Time between transmission and onset of infectiousness or symptoms	5 days	Furukawa et al. (2020); Hellewell et al. (2020); He et al. (2020); Lauer et al. (2020); Rong et al. (2020); Sanche et al. (2020)
f_A	Asymptomatic fraction	Fraction of infections which remain mild or asymptomatic	0.75*	Furukawa et al. (2020); Grassly et al. (2020); Liu et al. (2020a); Walsh et al. (2020); Widders et al. (2020)
f_Y	Severely symptomatic fraction	Fraction of infections which become severe and symptomatic	$1 - f_A^*$	-
$1/r$	Infectious period	Average time over which infected individuals can actively transmit the virus	8 days	Walsh et al. (2020); Widders et al. (2020)
Z	Population size	Total number of hosts (assumed fixed)	50000	Assumed

Table 1: Model parameter definitions and baseline numerical values used. Values for highly uncertain parameters based on the current literature for which we make an estimate are indicated with an asterisk.

152 rate model $\dot{T}(t) = \gamma P(t)$, where γ represents a testing rate parameter, is insufficient for describing
153 resource-limited scenarios. Under a linear model, even if γ is made to be very small in reflection of
154 testing limitations, the rate at which tests are administered will always increase in proportion with

155 the demand for testing, and this can not describe a resource-limited scenario where the maximum
156 testing rate is capped at a fixed value independent of the testing demand. The linear model is
157 in fact equivalent to our testing model in Eq. (2) under the testing time-limited regime shown in
158 Eq. (3), which represents a resource-rich rather than resource-limited scenario.

159 We note further that the testing rate model in Eq. (2) can be extended to multiple sub-
160 populations subject to distinct testing capacity constraints. Specifically, suppose two distinct sub-
161 populations $P_1(t)$ and $P_2(t)$ are subject to two distinct testing policies with distinct resource pools
162 limited by the capacities C_1 and C_2 , respectively. In this scenario, the total rate at which tests are
163 administered to the two populations is given by the following:

$$\dot{T}(t) = \frac{P_1(t)}{\tau + \frac{P_1(t)}{C_1 Z}} + \frac{P_2(t)}{\tau + \frac{P_2(t)}{C_2 Z}}. \quad (4)$$

164 **Disease model with resource allocation, contact tracing, and quarantine**

165 We now utilize our testing model to incorporate a quarantine and contact tracing program into our
166 disease model. We assume that testing resources can be allocated between two control strategies,
167 designated “clinical testing” and “non-clinical testing,” which are applied to individuals based the
168 presence of observable symptoms. Clinical testing applies resources to the moderate to severely
169 symptomatic class $Y(t)$. This strategy represents saving resources for hospital and health care
170 facilities to ensure adequate treatment of the most seriously ill individuals. Under a pure clinical
171 testing strategy, individuals are only eligible to be tested if they show severe enough symptoms.
172 Non-clinical testing applies resources to the exposed class $E(t)$ and the asymptomatic class $A(t)$,
173 as well as to some portion of the uninfected population. This strategy represents a combination
174 of contact tracing and population monitoring designed to identify asymptomatic individuals before
175 they can transmit the disease. For both strategies, we assume perfectly accurate tests with no
176 false positives or negatives, and we assume that testing can detect the disease at any point after
177 infection to when the period of infectiousness ends. These assumptions are somewhat optimistic
178 in comparison to real-world testing efficacies (Kucirka et al., 2020; Surkova et al., 2020), and our
179 model thus represents a limit on what can be achieved.

180 When an infected individual is tested in our model, they will instantly transition to the quar-
181 antine class $Q(t)$, and will subsequently recover from the disease and transition to the recovered

182 class. We also introduce the “unknown status” class $U(t)$, which is the subset of recovered hosts
183 who did not receive any testing or quarantine, and are therefore unaware that they previously had
184 COVID-19. We assume that the contact tracing and monitoring programs modeled by non-clinical
185 testing cover the entirety of the $E(t)$ and $A(t)$ classes, and some fraction $(1 - \eta)$ of the $S(t) + U(t)$
186 class, where $\eta \in [0, 1]$ denotes the “information parameter.” The value of η represents the quality of
187 information gained through contact tracing and case investigations, where larger η represents better
188 information, and the quantity $(1 - \eta)(S(t) + U(t))$ gives the fraction of the COVID-19 negative
189 population with an unknown infection history which will be targeted under non-clinical testing. In
190 other words, with better information, more non-clinical testing resources will be used for quaran-
191 tining the COVID-19 positive population, and less will be “wasted” obtaining negative results. The
192 case $\eta = 1$ represents perfect contact tracing and case investigation, where all non-clinical testing
193 is focused on infected individuals. While this extreme is unrealistic, η values close to 1 may be
194 plausible given high quality contact information and well-understood disease dynamics. The case
195 $\eta = 0$ represents no information such that non-clinical testing is randomly dispersed among the
196 non-symptomatic infected classes and the entirety of the $S(t) + U(t)$ classes, and thus represents a
197 large scale population monitoring program.

198 Suppose that a fraction ρ of the testing capacity C is allocated to non-clinical testing, with
199 the remainder devoted to clinical testing. The parameter ρ denotes the “strategy parameter,” and
200 its value represents a government’s policy for balancing health care resources between reservation
201 for more critical symptomatic cases and for use in contact tracing or monitoring programs. Our
202 modified SEIR model including testing, contact tracing, quarantine, and resource allocation is as

203 follows:

$$\dot{S}(t) = -\lambda_A \beta \frac{A(t)}{Z} S(t) - \lambda_Y \beta \frac{Y(t)}{Z} S(t) \quad (5a)$$

$$\dot{E}(t) = \lambda_A \beta \frac{A(t)}{Z} S(t) + \lambda_Y \beta \frac{Y(t)}{Z} S(t) - \varepsilon E(t) - \frac{E(t)}{\tau + \frac{E(t)+A(t)+(1-\eta)(S(t)+U(t))}{\rho CZ}} \quad (5b)$$

$$\dot{A}(t) = f_A \varepsilon E(t) - rA(t) - \frac{A(t)}{\tau + \frac{E(t)+A(t)+(1-\eta)(S(t)+U(t))}{\rho CZ}} \quad (5c)$$

$$\dot{Y}(t) = f_Y \varepsilon E(t) - rY(t) - \frac{Y(t)}{\tau + \frac{Y(t)}{(1-\rho)CZ}} \quad (5d)$$

$$\dot{Q}(t) = \frac{E(t) + A(t)}{\tau + \frac{E(t)+A(t)+(1-\eta)(S(t)+U(t))}{\rho CZ}} + \frac{Y(t)}{\tau + \frac{Y(t)}{(1-\rho)CZ}} - rQ(t) \quad (5e)$$

$$\dot{R}(t) = rA(t) + rY(t) + rQ(t) \quad (5f)$$

$$\dot{U}(t) = rA(t) + rY(t). \quad (5g)$$

204 Note that as $\rho \rightarrow 1$, Eq. (5d) reduces to Eq. (1d), and as $\rho \rightarrow 0$, Eqs. (5b) and (5c) reduce to
 205 Eqs. (1b) and (1c), respectively. Additionally, as $C \rightarrow 0$, all of Eq. (5) reduces to Eq. (1). In the
 206 [Appendix](#), we analyze a closed-form expression for R_0 under our full SEIR + testing and quarantine
 207 model.

208 A summary of all control related parameters is given in Table 2 for reference. For all simulations,
 209 we assume the testing time $\tau = 1$ day, which is reasonable for an effective testing and processing
 210 system lacking patient backlogs. For all other control parameters, we will consider a range of
 211 numerical values. Note that for notational simplicity in our model equations, we define C in units
 212 of tests per person per day, while actual testing capacities are often reported in units of tests per
 213 thousand people per day. To establish clear connections between our results and real-world testing
 214 limitations, we too report numerical values for testing capacity in units of tests per thousand per
 215 day. Thus, if we report a particular numerical value C_{1K} in per thousand units, the corresponding
 216 value in per person units used for numerical simulations is given by $C_{1K}/1000$.

217 **Flattening the epidemic peak as a control goal**

218 In accordance with the goal of “flattening the curve” typically communicated by government and
 219 health agencies ([World Health Organization, 2020a](#)), we simulate our model dynamics to determine

Parameter	Name	Meaning
C	Testing capacity	Maximum number of test able to be administered per day per capita
τ	Testing time	Average amount of time required for an individual be tested (including procrastination, travel time, processing time, etc.) absent of backlogs or delays due to other patients
ρ	Strategy parameter	Fraction of testing capacity used for non-clinical testing
η	Information parameter	$(1 - \eta)$ = fraction of COVID-19 negative population with unknown infection history targeted by non-clinical testing

Table 2: Testing and quarantine control parameter definitions

220 if and to what extent appropriately allocated resources can reduce the peak number of infections.
 221 First, we calculate optimal resource allocation strategies ρ for reducing the epidemic peak (defined
 222 as the maximum value of the sum of the E , A , and Y classes), assuming parameter values in Table
 223 1 and an initial outbreak of one exposed individual as our baseline case. Optimization is executed
 224 by numerically integrating the disease dynamics in Eq. (5) and utilizing the *fmincon* function in
 225 *MatlabR2017a* running the *sqp* algorithm with $\rho = 0$ as an initial guess. To account for the possi-
 226 bility of multiple local minima, we employ the parallel *MultiStart* algorithm from *Matlab's* global
 227 optimization toolbox. Simulations assume specific values values for η and find optimal ρ and epi-
 228 demic peak values for all testing capacities in the range $[0, 25]$ (in units of tests per thousand per
 229 day). In the [Appendix](#), we consider the alternative optimization goal of minimizing R_0 under our
 230 combined disease + testing model.

231 To determine the effects of delays in testing/quarantine policy implementation, as well as the
 232 effects of social distancing efforts, we consider alternative scenarios of initial conditions and/or
 233 model parameters. We model implementation delays by considering initial conditions equal to the
 234 outbreak size after a given number days under our baseline scenario with no testing or quarantine
 235 controls. In the case of a 30 day delay, for example, the alternative initial condition is given by
 236 $(S(0), E(0), A(0), Y(0), R(0)) = (49727, 134, 63, 21, 55)$, which yields 218 initially infected individ-
 237 uals. To model the effects of social distancing, we reduce β to a given fraction of its baseline value.
 238 Additionally, we consider the effects of social distancing and implementation delays together. To

239 evaluate the effects of alternative scenarios on optimal control policies, we perform the same op-
240 timization procedure as in our baseline case. We provide an in-depth examination of the specific
241 conditions of a 30 day initial testing delay and a 50% reduction of β , and also consider a broader
242 range of delays and β reductions in less detail.

243 Results

244 Optimal resource allocation strategies

245 We find that, even under extremely limited testing capacities, the epidemic peak can be reduced
246 to the initial outbreak size of 1 infected individual, provided that resources are optimally allocated
247 and sufficient information quality is available (Fig. 1a). Reducing the epidemic peak to the initial
248 outbreak size signifies that disease spread has been effectively suppressed. For a given η at low
249 testing capacities, the optimal strategy is to devote all resources to clinical testing, and a minimum
250 threshold capacity $C^{th}(\eta)$ exists, above which optimal strategies call for a mix of clinical and non-
251 clinical testing (Fig. 1b). As testing capacity increases above $C^{th}(\eta)$ optimal strategies require
252 an increasing share of resources to be devoted to non-clinical testing until a second threshold
253 capacity $C^*(\eta)$ is reached. The threshold $C^*(\eta)$ represents the smallest testing capacity for which
254 the outbreak can be suppressed to its initial size with an information level η . For example, at
255 information level $\eta = 0.90$, $C^{th}(\eta) = 2.8$ and $C^*(\eta) = 15.4$ tests per thousand per day (Fig. 1b).
256 Table 3 summarizes the threshold capacity definitions and gives numerical values for various values
257 of η .

258 For testing capacities $C > C^*(\eta)$, the epidemic peak size will always be reduced to 1 as long
259 as at least as much of the total capacity is devoted to clinical and non-clinical testing as is called
260 for by the optimal strategy at $C = C^*(\eta)$. As a result, optimal strategies are not unique when
261 $C > C^*(\eta)$. To see this non-uniqueness explicitly, consider an information level η , and let $\rho^*(\eta)$
262 denote the optimal strategy parameter at the critical capacity $C^*(\eta)$. At this critical capacity, the
263 optimal action is to devote $\rho^*(\eta)C^*(\eta)$ total resources to non-clinical testing and $(1 - \rho^*(\eta))C^*(\eta)$
264 total resources to clinical testing, the result of which reduces the epidemic to the smallest possible
265 value 1. If the testing capacity C exceeds the critical level $C^*(\eta)$, one can always allocate at least
266 $\rho^*(\eta)C^*(\eta)$ and $(1 - \rho^*(\eta))C^*(\eta)$ total resources to non-clinical and clinical testing, respectively,

267 thereby guaranteeing the epidemic peak to be reduced to 1. The allocation of the remaining
268 $C - C^*(\eta)$ resources will therefore be irrelevant, as adding resources to either strategy can not
269 further decrease the peak size beyond the initial infection size. In other words, for a given η , if
270 $C > C^*(\eta)$, the epidemic peak will be reduced to 1 whenever ρ is selected such that $\rho C \geq \rho^*(\eta)C^*(\eta)$
271 and $(1 - \rho)C \geq (1 - \rho^*(\eta))C^*(\eta)$. These inequalities imply that any ρ drawn from the interval
272 $\left[\rho^*(\eta)\frac{C^*(\eta)}{C}, \rho^*(\eta)\frac{C^*(\eta)}{C} + \left(1 - \frac{C^*(\eta)}{C}\right)\right]$ will reduce that epidemic peak to the minimum possible
273 value, thus showing that the optimal strategy is not unique for $C > C^*(\eta)$.

274 For a given capacity C , there exists a critical information value $\eta^{crit}(C)$, below which the optimal
275 strategy is clinical testing only, and above which the optimal strategy is mixed (Fig. 1). From the
276 definition of $C^{th}(\eta)$ as the minimal capacity below which the optimal strategy is clinical testing only
277 for a given η , we have the relation $C^{th}(\eta_0) = C_0$ if and only if $\eta^{crit}(C_0) = \eta_0$, and numerical values for
278 $\eta^{crit}(C)$ at specific C values can therefore be inferred from Table 3. The critical information value
279 represents an important practical decision making threshold for public health officials operating
280 under a potentially limited testing capacity C ; if η is estimated to be below $\eta^{crit}(C)$, no testing
281 resources should be diverted away from severely symptomatic individuals, while if η is estimated
282 to be above $\eta^{crit}(C)$, important resource management decisions should be considered. In Fig. 2,
283 we plot η^{crit} as a function of testing capacity C . Here, the curve defined by $\eta^{crit}(C)$ divides the
284 (C, η) plane into two regimes, one where the optimal strategy calls for clinical testing only, one
285 where optimal strategies are a mix of clinical and non-clinical testing. In particular, we find that
286 for $C > 8.0$ tests per thousand per day, $\eta^{crit}(C) = 0$. Thus, for testing capacities above 8.0, it
287 is always optimal to devote at least some resources to non-clinical testing, even if the non-clinical
288 testing is a simple randomized population sampling program lacking the efficacy of targeted contact
289 tracing efforts.

Threshold Capacity	Definition	Numerical Values (tests per thousand per day)							
		$\eta = 0.00$	$\eta = 0.50$	$\eta = 0.85$	$\eta = 0.90$	$\eta = 0.95$	$\eta = 0.97$	$\eta = 0.999$	$\eta = 1.00$
$C^{th}(\eta)$	Minimal capacity beyond which optimal strategies are mixed	8.0	6.0	3.4	2.8	1.8	1.2	0.1	0.0
$C^*(\eta)$	Minimal capacity beyond which optimal strategies reduce epidemic peaks to initial infection levels	154.0	77.0	23.1	15.4	7.6	4.6	0.2	0.0

Table 3: Threshold testing capacity definitions and numerical values for the information levels η considered in Fig. 1. Note that critical information threshold levels $\eta^{crit}(C)$ can be inferred from this table from the relationship $C^{th}(\eta_0) = C_0$ if and only if $\eta^{crit}(C_0) = \eta_0$. For example, the $\eta = 0.90$ column indicates that $\eta^{crit}(2.8) = 0.90$.

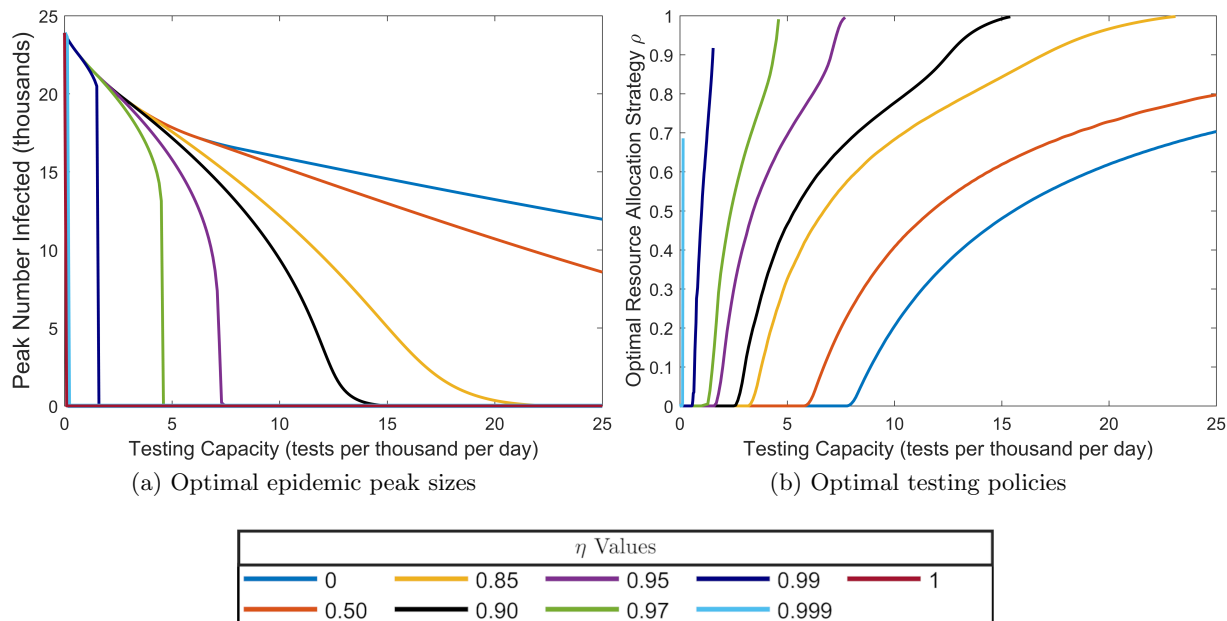


Figure 1: Optimally reduced epidemic peak sizes and corresponding optimal ρ values as a function of testing capacity. Note that the peak value 23,882 at zero testing capacity corresponds to the uncontrolled disease dynamics without a testing or quarantine program. **(a)** Optimally reduced epidemic peak sizes as a function of testing capacity for the values of non-symptomatic testing information quality η indicated in the legend. **(b)** Optimal resource allocation strategies ρ for reducing the epidemic peak as a function of testing capacity. An optimal ρ curve which terminates at a testing capacity C^* below than the maximally considered value 25.0 tests per thousand per day indicates an information level for which the optimal strategy is not unique at capacities above C^* , and for which the optimal epidemic peak size can be reduced to the initial value of one infected at capacities above C^* . Note that for perfect information $\eta = 1$, the optimal testing strategy is not unique down to the smallest non-zero testing capacity considered 0.01 tests per thousand per day. Note also that for $\eta = 0.85, 0.90, 0.95$, and 0.97 , the optimal ρ values at $C = C^*$ appear to be close to 1, but are not actually equal to 1.

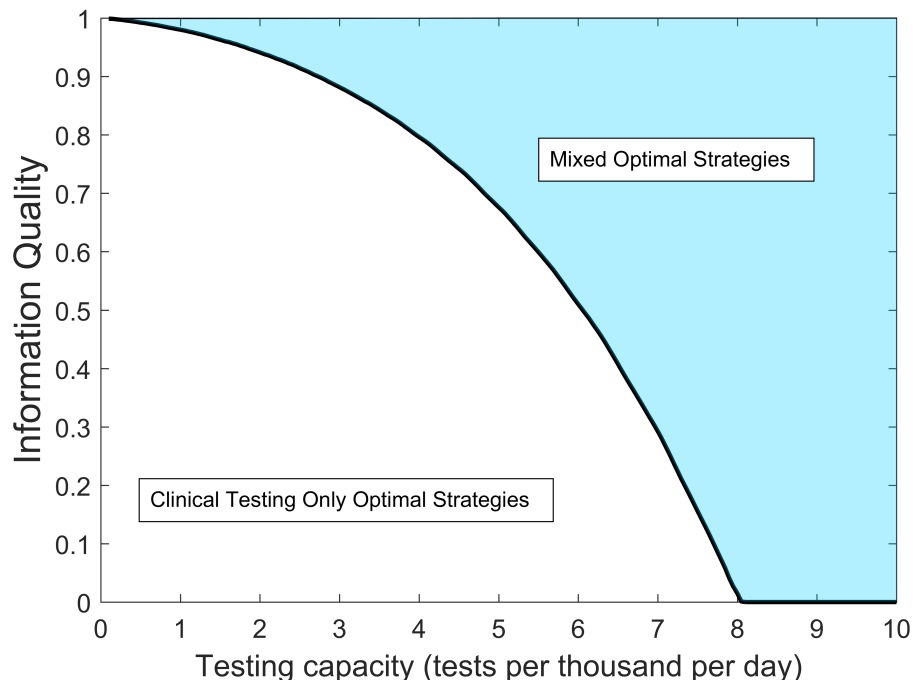


Figure 2: Optimal resource allocation strategy regimes for reducing the epidemic peak as a function of testing capacity C and non-clinical testing information quality η . For (C, η) values within the shaded region, optimal strategies call for sharing resources between a mix of clinical and non-clinical testing. Within the non-shaded region, optimal strategies call for all resources to be concentrated to clinical testing only. The black curve indicates a critical information threshold which for a given testing capacity, determines whether the optimal strategy will be mixed or clinical testing only.

290 Social distancing and delays in testing program implementation

291 Unsurprisingly, delaying the implementation of a testing program by 30 days has negative impact
292 on optimal peak reduction, with the delay being most detrimental at the lowest testing capacities
293 (cf. Figs 3a and 3b). Specifically, a delay of this magnitude makes it impossible to reduce the
294 epidemic peak to its initial value, regardless of the information level, within the range of testing
295 capacities $[0, 1.2]$ tests per thousand per day (Fig. 3a). This is not the case for immediate testing
296 program implementation, where the peak can be reduced to its initial value at *any* non-zero testing
297 capacity given sufficient information quality (Fig. 1). Reducing the peak to its initial value is an
298 important control goal, as it is equivalent to the ability to force an immediate downturn in the
299 infection curve upon implementation of testing and quarantine. These results emphasize the need
300 for early implementation of a testing program at the beginning stages of a novel disease epidemic,

301 where resources may be extremely limited as health agencies adjust to the biology of the newly
302 discovered infectious agent.

303 Halving the contact rate, which simulates the influence of social distancing, has a strong effect
304 on optimal policies and peak sizes (Figs. 3c and 3d). At zero testing capacity (which corresponds
305 to the disease dynamics without testing and quarantine), the epidemic peak reaches 11,669 indi-
306 viduals, which is approximately half of the no testing peak value without social distancing. This
307 finding is not surprising given that we model social distancing by reducing the contact rate β by
308 half. Generally, social distancing expands the range of testing capacities over which the peak can
309 be reduced to its initial value for a given information level. Compare, for example, the $\eta = 0.90$
310 curve in Fig. 3c to that of Fig. 1a. We thus conclude that social distancing allows for more effec-
311 tive utilization of limited testing capacities under lower information quality levels. Note that in
312 both the base and socially distanced parameter scenarios, we find no non-zero testing capacities for
313 which the peak can not be suppressed to its initial size for $\eta = 1$, and therefore no range of testing
314 capacities over which the optimal ρ is unique (Figs. 3d and 1b).

315 Combining the two modulating factors shows that the beneficial effects of social distancing at
316 low testing capacities can counteract some of the detrimental effects of delays in testing implemen-
317 tation (Figs. 3e and 3d). Indeed, social distancing reduces the testing capacity range over which
318 implementation delays render epidemic control impossible. This interval is given by $[0, 0.4]$ tests
319 per thousand per day with 50% contact reduction social distancing (Fig. 3e), as compared to $[0, 1.2]$
320 without social distancing (Fig. 3a). For all delays between 1 day and the time of the uncontrolled
321 epidemic peak, 62 days, larger degrees of contact reduction from social distancing yield larger re-
322 ductions in the range of testing capacities for which the peak can not be reduced to its initial size
323 under perfect information (Fig. 4). Note that after day 62, the infection curve turns downward in
324 the uncontrolled model, so for delays greater than 62 days in the controlled model, the epidemic
325 peak value will always be equal to the initial value regardless of testing capacity, and peak reduction
326 is not a useful control goal. In total, these results emphasize the importance of social distancing
327 during the early resource-limited stages of a novel disease epidemic.

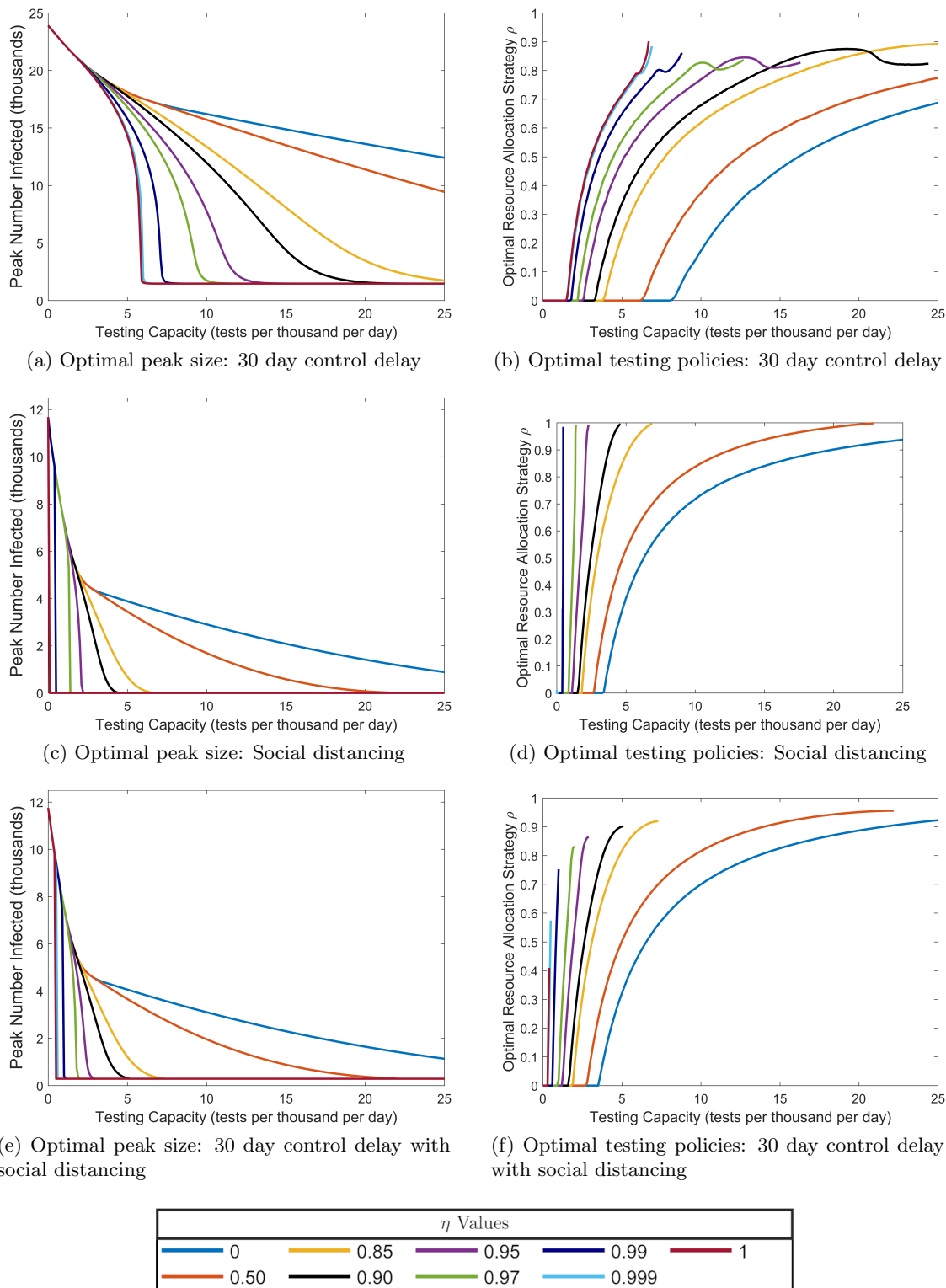


Figure 3: Effects of social distancing and control delays on optimal testing strategies for reducing the epidemic peak. See Fig. 1 for a comparison to our baseline case and an explanation of the meaning of each plot.

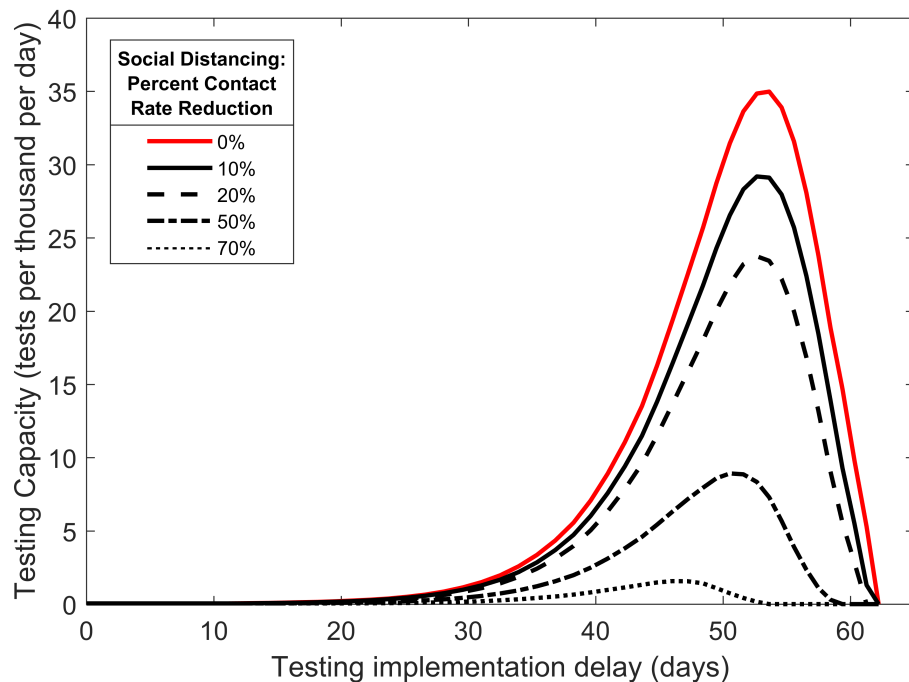


Figure 4: Combined effects of social distancing and delays in testing implementation on epidemic controlability. Threshold testing capacities are plotted as a function of implementation delay, where different curves represent different social distancing strengths as percent reduction in the contact rate. For a given implementation delay time, if testing capacity falls below the value indicated by a curve in the figure, the epidemic will not be forced into a downturn upon control implementation despite perfect information, assuming the indicated level of social distancing.

328 Discussion

329 The COVID-19 pandemic has exposed a critical lack of capacity for diagnostic testing in an emerg-
330 ing pandemic. Using a modified SEIR model, we explored how distributing a limited amount of
331 testing effort can affect the course of an epidemic when testing is directly coupled to quarantine.
332 The model is tailored to the epidemiology of SARS-CoV-2, and divides infected individuals into
333 symptomatic and non-symptomatic classes, with the latter class including individuals who have
334 been exposed but are not yet infectious as well as those who are infectious but not strongly symp-
335 tomatic. We further defined clinical testing as that focused exclusively on the symptomatic class,
336 while non-clinical testing is distributed across the rest of the potentially infected population (S, E,
337 A, and U). For a given testing capacity C , our model thus allows us to identify optimal testing
338 policies in terms of the balance between clinical and non-clinical testing, modulated by the strategy
339 parameter, ρ , and the information parameter η . This latter parameter governs the extent to which
340 non-clinical testing is concentrated on infected individuals. We further examined how optimal poli-
341 cies shift as a function of testing capacity.

342 Focusing on the goal of maximally reducing the height of the infection curve (i.e., “flattening
343 the curve”), we found that optimal testing is always able to suppress the epidemic, provided that
344 testing is implemented at the onset of disease transmission. Clinical testing strategies are gener-
345 ally optimal at low testing capacities. Under some conditions when the testing rate is low, mixed
346 strategies that include a small but finite amount of non-clinical testing are optimal, but only when
347 there is essentially perfect information with which to focus non-clinical testing on infected individ-
348 uals. While perfectly omniscient non-clinical testing is unlikely to be achieved in reality, high η
349 values may be possible with efficient contact tracing and case investigation programs. These results
350 therefore suggest that testing policies employed in many countries early in the pandemic, which
351 strongly emphasized clinical testing with some additional testing effort aimed at the highest risk
352 individuals (e.g., front-line healthcare workers), were reasonable. Furthermore, we demonstrated
353 that exclusively non-clinical testing is never the optimal strategy. In other words, non-clinical test-
354 ing plus a small but finite amount of clinical testing will always be better than a purely non-clinical
355 strategy for epidemic peak reduction.

356 Since the onset of the pandemic, testing capacity has steadily increased throughout much of

357 the world. Our results show that increased testing capacity brings with it a broader range of possi-
358 bilities for optimizing testing. As testing rate increases, the amount of proxy information required
359 for a mixed strategy to be optimal decreases, with all other factors held constant. At a testing
360 capacity of 8 tests per day per 1000 people, a mixed strategy becomes optimal even when there is
361 no proxy information available to pinpoint non-symptomatic infected individuals. This testing rate
362 thus defines the minimal testing capacity for which a broad, non-targeted population monitoring
363 program, in conjunction with clinical testing, is optimal. While on the higher end of the realistic
364 range of testing rates, this level of testing has been exceeded in several countries, including Den-
365 mark, Iceland, Luxembourg, and United Arab Emirates.

366 While we have chosen minimizing the height of the peak of the infection curve as a pragmatic
367 and meaningful control goal, we also explored the common approach of minimizing R_0 (see [Ap-](#)
368 [pendix](#)). A mathematical advantage of R_0 minimization is that it leads to closed-form expressions
369 for key threshold parameter values that delimit the conditions under which different testing strate-
370 gies are optimal. However, we found that for our model, results between these two control goals
371 often differed markedly. Specifically, we identified conditions under which testing policies resulting
372 in $R_0 < 1$ still yielded large outbreaks, which suggests limited utility of R_0 as a control target.
373 We hypothesize that this phenomenon results from the combination of a finite system size and
374 a finitely small initial condition (see [Appendix](#)). We further note that the choice of control goal
375 can also lead to qualitatively different conclusions about optimal strategies. For example, purely
376 clinical testing strategies are never optimal under R_0 minimization, which contrasts sharply with
377 low testing capacity results for peak minimization.

378 Our results suggest that testing early is critically important to control efforts. Specifically, the
379 range of testing rates that allows full epidemic control is broadest when testing is implemented im-
380 mediately at the start of an epidemic. A delay of even 30 days is sufficient to significantly narrow the
381 conditions under which the epidemic can be brought to heel. Looking in the other direction, miti-
382 gation efforts that lower the effective contact rate, such as lockdowns, social distancing, and mask
383 wearing, significantly facilitate epidemic control, particularly when combined with early testing.
384 Importantly, interventions that reduce the contact rate also lower the threshold testing capacity
385 where uniform random testing of the non-symptomatic population is warranted. These consid-
386 erations suggest that testing programs should be designed in conjunction with non-pharmaceutical

387 interventions.

388 Taken together, our results suggest that focusing exclusively or mostly on clinical testing at
389 very low testing capacities is often optimal or close to optimal. As testing capacities increase,
390 which can typically be expected to happen with time since epidemic onset, the options for opti-
391 mally distributing testing effort also open up. To our knowledge, this possibility has been largely
392 unexplored in the literature. This implies that the main gains to be had by optimizing allocation
393 of testing effort will occur at intermediate testing capacities, where options exist for optimization,
394 but capacity is still limited relative to demand. These considerations further suggest that testing
395 policies should evolve over time, and that time-dependent optimal control (Kirk, 1998; Lenhart
396 and Workman, 2007), which can explicitly account for the dynamics of testing capacity, will be
397 necessary to robustly identify how testing should change through the course of an epidemic. While
398 beyond the scope of the present effort, broadening our approach to consider time-depenent optimal
399 control is a clear next step. Another key direction for future efforts would be to consider optimal
400 allocation of testing effort after relaxing the homogeneous, well-mixed population assumption at the
401 core of compartment-type disease models. Spaially explicit extensions of disease models have been
402 shown to change key quantities such as immunization thresholds (Eisinger and Thulke, 2008), and
403 we expect that introducing spatial heterogeneity would also change the picture for optimal testing.

404 **Acknowledgements**

405 This work was partially funded by the Center of Advanced Systems Understanding (CASUS) which
406 is financed by Germany’s Federal Ministry of Education and Research (BMBF) and by the Saxon
407 Ministry for Science, Culture and Tourism (SMWK) with tax funds on the basis of the budget
408 approved by the Saxon State Parliament. This work was also partially funded by the Where2Test
409 project, which is financed by SMWK with tax funds on the basis of the budget approved by the
410 Saxon State Parliament.

411 **Appendix**

412 In this appendix, we provide an analytic expression for our model’s basic reproduction number, R_0 ,
413 and we demonstrate that R_0 reduction is not a reliable metric of control efficacy for epidemic peak

414 reduction. The basic reproduction number is a threshold quantity which determines the stability of
415 a disease-free population with no natural or acquired immunity: small numbers of initial cases will
416 produce large epidemic outbreaks when $R_0 > 1$, and will result in rapid disease die-out when $R_0 < 1$
417 (Diekmann et al., 1990). Intuitively, R_0 quantifies the number of secondary cases produced by a
418 typical initial case when interacting with the disease-free state. Because we are able to obtain an
419 analytic expression for R_0 , the question of its suitability as a metric for control efficacy is especially
420 prescient; the ability to analytically minimize R_0 rather than numerically minimize the peak itself
421 would provide exact expressions and deep mechanistic insight into optimal control strategies if R_0
422 were indeed found to be a reliable metric for control efficacy.

423 Analytic expression for R_0

424 The analytic expression for our model's basic reproduction number is found utilizing the next-
425 generation matrix method (van den Driessche and Watmough, 2002). We find that R_0 can in-
426 terpreted as the asymptomatic population fraction f_A multiplied by average number of secondary
427 infectious individuals produced by an asymptomatic case, plus the symptomatic population frac-
428 tion f_Y multiplied by the average number of secondary infectious individuals produced by an
429 symptomatic case:

$$R_0 = f_A \frac{\varepsilon}{V_E} \frac{\lambda_A \beta}{V_A} + f_Y \frac{\varepsilon}{V_E} \frac{\lambda_Y \beta}{V_Y}, \quad (6)$$

430 where

$$V_E = \begin{cases} \varepsilon, & C = 0 \\ \varepsilon, & C \neq 0, \rho = 0 \\ \varepsilon + \frac{1}{\tau + \frac{1-\eta}{\rho C}}, & C \neq 0, \rho \neq 0, \end{cases} \quad (7)$$

431

$$V_A = \begin{cases} r, & C = 0 \\ r, & C \neq 0, \rho = 0 \\ r + \frac{1}{\tau + \frac{1-\eta}{\rho C}}, & C \neq 0, \rho \neq 0, \end{cases} \quad (8)$$

432

$$V_Y = \begin{cases} r, & C = 0 \\ r, & C \neq 0, \rho = 1 \\ r + \frac{1}{\tau}, & C \neq 0, \rho \neq 1. \end{cases} \quad (9)$$

433 The case $C = 0$ corresponds to the uncontrolled model in Eq. (1), and R_0 is a discontinuous
 434 function of C at $C = 0$ except for the special case $\rho = 1, \eta = 1$. Under uncontrolled conditions, the
 435 parameters in Table 1 give an $R_0 = 5.0$, with 3.0 originating from the asymptomatic contribution,
 436 and 2.0 originating from the symptomatic contribution. For $C \neq 0$, R_0 is a discontinuous function
 437 of ρ at $\rho = 1$ and at $\rho = 0, \eta = 1$. Note that these discontinuous limits represent potentially
 438 unrealistic extremes of testing policies and information quality.

439 Suitability of R_0 as a control metric

440 To determine if R_0 reduction provides a reliable assessment of control efficacy for epidemic peak
 441 reduction, we plot the peak size as a function of R_0 in Fig. 5. These figures were generated by
 442 integrating Eq. (5) for specific C and η and all $\rho \in [0, 1]$ assuming the baseline parameter values
 443 and initial condition, and plotting the resulting peak values against the corresponding R_0 values
 444 as determined by Eq. (6). These results show clearly that R_0 is not a reliable measure of control
 445 efficacy for epidemic peak reduction, as there exists several cases where the epidemic peak value
 446 increases as R_0 decreases. Further, there exist conditions where epidemic peaks are large even
 447 though $R_0 < 1$, in apparent contradiction the definition of $R_0 = 1$ as a threshold for large epidemic
 448 outbreaks. This effect can be seen in for $\eta = 1, 0.97$, and 0.95 in Fig. 5a, and for $\eta = 1$ and 0.97 in
 449 Fig. 5b. For $\eta = 0.97$ and 0.99 curves, large peaks occurring with $R_0 < 1$ correspond to ρ values
 450 very close but not equal to 1, while for the $\eta = 1$ curve, correspond ρ values very close but not

451 equal to 0.

452 To explain the presence of large outbreaks when $R_0 < 1$, we define the *effective testing time*,
453 τ_{eff} , which represents the average time an individual must wait to be tested given the current
454 backlog of patients. For the basic testing model in Eq. (2), the effective testing time is defined by
455 $\tau_{eff} = P(t)/\dot{T}(t)$, which evaluates to

$$\tau_{eff} = \tau + \frac{P(t)}{CZ}. \quad (10)$$

456 Extending this definition to our disease model with testing and quarantine in Eq. (5), we find two
457 effective testing times for non-clinical and clinical testing, denoted τ_{eff}^N and τ_{eff}^C , respectively:

$$\tau_{eff}^N = \tau + \frac{E(t) + A(t) + (1 - \eta)(S(t) + U(t))}{\rho CZ} \quad (11)$$

$$\tau_{eff}^C = \tau + \frac{Y(t)}{(1 - \rho)CZ}. \quad (12)$$

458 These effective testing times represent the average delays for asymptomatic and symptomatic in-
459 dividuals, respectively, in getting tested, receiving results, and moving to quarantine, given the
460 current backlog of patients and tests. τ_{eff}^N and τ_{eff}^C provide measures of non-clinical and clinical
461 control efficiency, respectively, under the current load of infected patients. Specifically, τ_{eff}^N and
462 τ_{eff}^C increase monotonically with the patient load (and are thus equal to the minimal possible test-
463 ing times when the patient load is negligibly small), so for larger patient loads, a fixed number of
464 resources will move individuals to quarantine at a slower effective per-capita rate. In this sense,
465 lower patient loads allow a given number of resources to be leveraged more efficiently.

466 We hypothesize that the large outbreaks observed when $R_0 < 1$ arise due to a finite system
467 size and a finitely small initial condition size. The threshold property of $R_0 = 1$ for outbreak
468 suppression assumes a disease-free equilibrium background state perturbed by a sufficiently small
469 number of initial infected individuals, where “sufficiently small” means small in comparison to the
470 total system size such that the disease dynamics can be well-approximated by linearizing about the
471 disease-free equilibrium. Under disease-free equilibrium conditions, there is no backlog of patients
472 needing to be tested, so the effective testing times in Eqs. (11) and (12) achieve their min-
473 imal values, and R_0 thus assumes a maximally efficient level of control when assessing outbreak

474 potential. Under the full disease dynamics, however, Eqs. (11) and (12) show that small numbers
 475 of initial infectives will produce slightly longer than minimal effective testing times, and that this
 476 small increase can become exaggerated when ρ is very close but not equal to 1 or 0. Thus, initial
 477 conditions can yield testing efficacies much smaller than those assumed by R_0 , sometimes to a
 478 degree which allows epidemics to grow even when $R_0 < 1$. In support of our hypothesis, we have
 479 found that reducing the initial condition size by a factor of 10 (which corresponds to less than one
 480 infected individual) eliminates the effect of large peaks when $R_0 < 1$ for all cases pictured in Fig. 5.

481

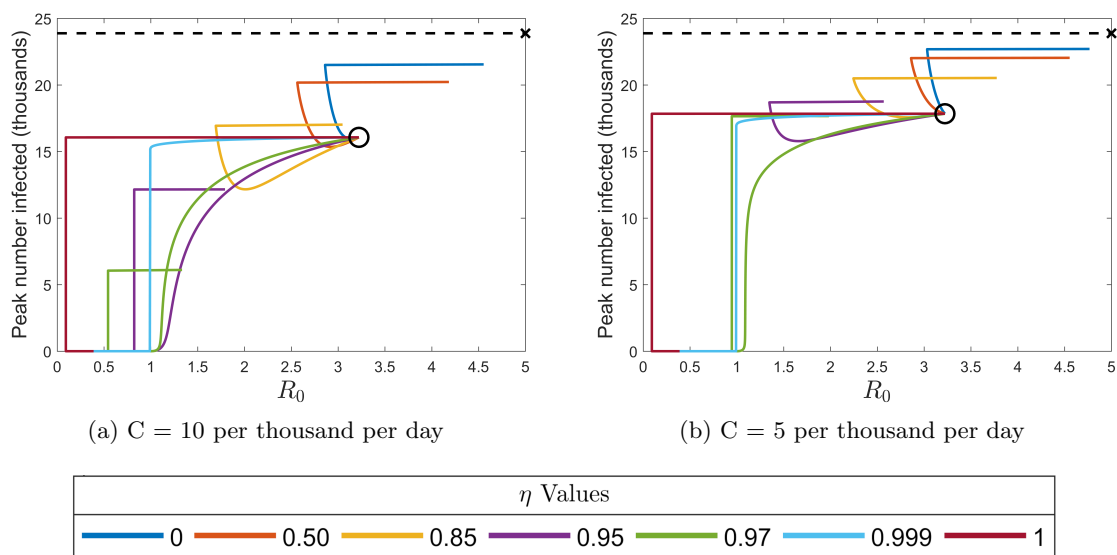


Figure 5: Epidemic peak values plotted as a function of R_0 for testing capacities $C = 10$ and $C = 5$ tests per thousand per day. Curve colors correspond to the information values η indicated in the legend. Along each curve, ρ increases from 0 and 1, with the beginning of each curve at $\rho = 0$ indicated by the centers of the black circles ($\rho = 0$ represents clinical testing only where the information parameter is irrelevant, so all curves must coincide). The dashed black lines indicate the uncontrolled peak value of 23882 infected individuals, and the black \times indicates the uncontrolled $R_0 = 5.0$.

482 References

- 483 Adhikari, K., Gautam, R., Pokharel, A., Uprety, K. N., and Vaidya, N. K. (2021). Transmission
484 dynamics of COVID-19 in Nepal: Mathematical model uncovering effective controls. *J. Theor.*
485 *Biol.*, 521:110680.
- 486 Ahmed, I., Modu, G. U., Yusuf, A., Kumam, P., and Yusuf, I. (2021). A mathematical model
487 of Coronavirus Disease (COVID-19) containing asymptomatic and symptomatic classes. *Results*
488 *Phys.*, 21:103776.
- 489 Aldila, D., Ndi, M. Z., and Samiadji, B. M. (2020). Optimal control on COVID-19 eradication
490 program in indonesia under the effect of community awareness. *Math. Biosci. Eng.*, 17:6355 –
491 6389.
- 492 Alvarez, F. E., Argente, D., and Lippi, F. (2020). A simple planning problem for COVID-19
493 lockdown. Working Paper 26981, National Bureau of Economic Research. Series: Working Paper
494 Series.
- 495 Amaku, M., Covas, D. T., Bezerra Coutinho, F. A., Azevedo Neto, R. S., Struchiner, C., Wilder-
496 Smith, A., and Massad, E. (2021). Modelling the test, trace and quarantine strategy to control
497 the COVID-19 epidemic in the state of São Paulo, Brazil. *Infect. Dis. Model.*, 6:46–55.
- 498 Aragón-Caqueo, D., Fernández-Salinas, J., and Laroze, D. (2020). Optimization of group size
499 in pool testing strategy for SARS-CoV-2: A simple mathematical model. *Journal of Medical*
500 *Virology*, 92:1988–1994.
- 501 Centers for Disease Control and Prevention (2020). Interim guidance on developing a
502 COVID-19 case investigation and contact tracing plan. [cited 2020 September 23]. Avail-
503 able from: [https://www.cdc.gov/coronavirus/2019-ncov/php/contact-tracing/contact-tracing-](https://www.cdc.gov/coronavirus/2019-ncov/php/contact-tracing/contact-tracing-plan/overview.html)
504 [plan/overview.html](https://www.cdc.gov/coronavirus/2019-ncov/php/contact-tracing/contact-tracing-plan/overview.html).
- 505 Chatzimanolakis, M., Weber, P., Arampatzis, G., Wälchli, D., Karnakov, P., Kičić, I., Papadim-
506 itriou, C., and Koumoutsakos, P. (2020). Optimal Testing Strategy for the Identification of
507 COVID-19 Infections. *medRxiv*. Publisher: Cold Spring Harbor Laboratory Press.

- 508 Choi, W. and Shim, E. (2021). Optimal strategies for social distancing and testing to control
509 COVID-19. *J. Theor. Biol.*, 512:110568.
- 510 Cleevly, M., Susskind, D., Vines, D., Vines, L., and Wills, S. (2020). A workable strategy for Covid-
511 19 testing: Stratified periodic testing rather than universal random testing. *Covid Economics*,
512 (8):44.
- 513 Contreras, S., Villavicencio, H. A., Medina-Ortiz, D., Biron-Lattes, J. P., and Olivera-Nappa,
514 A. (2020). A multi-group SEIRA model for the spread of COVID-19 among heterogeneous
515 populations. *Chaos Solitons Fractals*, 136:109925.
- 516 de Wolff, T., Pflüger, D., Rehme, M., Heuer, J., and Bittner, M.-I. (2020). Evaluation of Pool-
517 based Testing Approaches to Enable Population-wide Screening for COVID-19. *arXiv:2004.11851*
518 [*q-bio, stat*]. arXiv: 2004.11851.
- 519 Diekmann, O., Heesterbeek, J. A. P., and Metz, J. A. J. (1990). On the definition and the com-
520 putation of the basic reproduction ratio R_0 in models for infectious diseases in heterogeneous
521 populations. *Journal of Mathematical Biology*, 28:365 – 382.
- 522 Dwomoh, D., Iddi, S., Adu, B., Aheto, J. M., Sedzro, K. M., Fobil, J., and Bosomprah, S. (2021).
523 Mathematical modeling of COVID-19 infection dynamics in Ghana: Impact evaluation of inte-
524 grated government and individual level interventions. *Infect. Dis. Model.*, 6:381–397.
- 525 Eisinger, D. and Thulke, H.-H. (2008). Spatial pattern formation facilitates eradication of infectious
526 diseases. *Journal of Applied Ecology*, 45(2):415–423.
- 527 Emanuel, E. J., Persad, G., Upshur, R., Thome, B., Parker, M., Glickman, A., Zhang, C., Boyle,
528 C., Smith, M., and Phillips, J. P. (2020). Fair allocation of scarce medical resources in the time
529 of Covid-19. *New England Journal of Medicine*, 382:2049–2055.
- 530 Furukawa, N. W., Brooks, J. T., and Sobel, J. (2020). Evidence supporting transmission of severe
531 acute respiratory syndrome coronavirus 2 while presymptomatic or asymptomatic. *Emerging*
532 *Infectious Diseases*, 26:e201595.
- 533 Ghosh, S., Rajwade, A., Krishna, S., Gopalkrishnan, N., Schaus, T. E., Chakravarthy, A., Varahan,
534 S., Appu, V., Ramakrishnan, R., Ch, S., Jindal, M., Bhupathi, V., Gupta, A., Jain, A., Agarwal,

- 535 R., Pathak, S., Rehan, M. A., Consul, S., Gupta, Y., Gupta, N., Agarwal, P., Goyal, R., Sagar,
536 V., Ramakrishnan, U., Krishna, S., Yin, P., Palakodeti, D., and Gopalkrishnan, M. (2020).
537 Tapestry: A Single-Round Smart Pooling Technique for COVID-19 Testing. preprint, Infectious
538 Diseases (except HIV/AIDS).
- 539 Gollier, C. and Gossner, O. (2020). Group testing against Covid-19. *Covid Economics*, 1(2):32 –
540 42. Publisher: CEPR Press.
- 541 Gonzalez-Reiche, A. S., Hernandez, M. M., Sullivan, M. J., Ciferri, B., Alshammery, H., Obla,
542 A., Fabre, S., Kleiner, G., Polanco, J., Khan, Z., Albuquerque, B., van de Guchte, A., Dutta,
543 J., Francoeur, N., Melo, B. S., Oussenko, I., Deikus, G., Soto, J., Sridhar, S. H., Wang, Y.-
544 C., Twyman, K., Kasarskis, A., Altman, D. R., Smith, M., Sebra, R., Aberg, J., Krammer,
545 F., García-Sastre, A., Luksza, M., Patel, G., Paniz-Mondolfi, A., Gitman, M., Sordillo, E. M.,
546 Simon, V., and van Bakel, H. (2020). Introductions and early spread of SARS-CoV-2 in the New
547 York City area. *Science*, 369:297–301.
- 548 Grassly, N., Pons Salort, M., Parker, E., White, P., Ainslie, K., Baguelin, M., Bhatt, S., Boonyasiri,
549 A., Boyd, O., Brazeau, N., and others (2020). Report 16: Role of testing in COVID-19 control.
550 *Imperial College London*.
- 551 Hansen, E. and Day, T. (2011). Optimal control of epidemics with limited resources. *Journal of*
552 *Mathematical Biology*, 62:423 – 451.
- 553 Hasell, J., Mathieu, E., Beltekian, D., Macdonald, B., Giattino, C., Ortiz-Ospina, E., Roser, M.,
554 and Ritchie, H. (2020). A cross-country database of covid-19 testing. *Scientific Data*, 7(1):1–7.
- 555 He, X., Lau, E. H. Y., Peng, W., Deng, X., Wang, J., et al. (2020). Temporal dynamics in viral
556 shedding and transmissibility of COVID-19. *Nature Medicine*, 26:672 –675.
- 557 Hellewell, J., Gimma, A. and Bosse, N. I., Jarvis, C. I., Munday, J. D., et al. (2020). Feasibility of
558 controlling COVID-19 outbreaks by isolation of cases and contacts. *Lancet Glob Health*, 8:e488
559 – e496.
- 560 Hussain, T., Ozair, M., Ali, F., Rehman, S. u., Assiri, T. A., and Mahmoud, E. E. (2021). Sensitivity

- 561 analysis and optimal control of COVID-19 dynamics based on SEIQR model. *Results Phys.*,
562 22:103956.
- 563 Jiang, S., Li, Q., Li, C., Liu, S., Wang, T., et al. (2020). Mathematical models for devising the
564 optimal SARS-CoV-2 strategy for eradication in China, South Korea, and Italy. *Journal of*
565 *Translational Medicine*, 18:345.
- 566 Jones, C. J., Philippon, T., and Venkateswaran, V. (2020). Optimal mitigation policies in a pan-
567 demic: Social distancing and working from home. Working Paper 26984, National Bureau of
568 Economic Research. Series: Working Paper Series.
- 569 Jonnerby, J., Lazos, P., Lock, E., Marmolejo-Cossío, F., Ramsey, C. B., Shukla, M., and Sridhar,
570 D. (2020). Maximising the benefits of an acutely limited number of COVID-19 tests. *arXiv*
571 *preprint arXiv:2004.13650*.
- 572 Khatua, D., De, A., Kar, S., Samanta, E., and Mandal, S. M. (2020). A dynamic optimal control
573 model for SARS-CoV-2 in India. Available at SSRN: <https://ssrn.com/abstract=3597498>.
- 574 Kirk, D. E. (1998). *Optimal Control Theory: An Introduction*. Dover Publications, Inc., Mineola,
575 New York.
- 576 Kretzschmar, M. E., Rozhnova, G., Bootsma, M. C. J., van Boven, M., van de Wijgert, J. H. H. M.,
577 and Bonten, M. J. M. (2020). Impact of delays on effectiveness of contact tracing strategies for
578 COVID-19: A modelling study. *Lancet Public Health*, 5:E452 – E459.
- 579 Kucirka, L. M., Lauer, S. A., Laeyendecker, O., Boon, D., and Lessler, J. (2020). Variation in
580 false-negative rate of reverse transcription polymerase chain reaction-based SARS-CoV-2 tests
581 by time since exposure. *Annals of Internal Medicine*, 173:262 – 267.
- 582 Lauer, S. A., Grantz, K. H., Bi, Q., and Jones, F. K. (2020). The incubation period of coronavirus
583 disease 2019 (COVID-19) from publically reported confirmed cases: Estimation and application.
584 *Annals of Internal Medicine*, 172:577 – 582.
- 585 Lenhart, S. and Workman, J. T. (2007). *Optimal Control Applied to Biological Models*. Chapman
586 and Hall/CRC, Boca Raton, Fl.

- 587 Li, R., Pei, S., Chen, B., Song, Y., Zhang, T., Yang, W., and Shaman, J. (2020). Substantial
588 undocumented infection facilitates the rapid dissemination of novel coronavirus (SARS-CoV-2).
589 *Science*, 368(6490):489–493.
- 590 Liu, Y., Yan, L., Wan, L., Xiang, T., Le, A., et al. (2020a). Viral dynamics in mild and severe
591 cases of COVID-19. *Lancet Infectious Diseases*, 20:656 – 657.
- 592 Liu, Z., Magal, P., Seydi, O., and Webb, G. (2020b). A COVID-19 epidemic model with latency
593 period. *Infectious Disease Modelling*, 5:323 – 337.
- 594 Majumder, M. S. and Mandl, K. D. (2020). Early in the epidemic: Impact of preprints on global
595 discourse about COVID-19 transmissibility. *Lancet Global Health*, 8:e627 – e630.
- 596 Ngonghala, C. N., Iboi, E., Eikenberry, S., Scotch, M., MacIntyre, C. R., Bonds, M. H., and Gumel,
597 A. B. (2020). Mathematical assessment of the impact of non-pharmaceutical interventions on
598 curtailing the 2019 novel Coronavirus. *Math. Biosci.*, 325:108364.
- 599 Piasecki, T., Mucha, P. B., and Rosińska, M. (2020). A new SEIR type model including quarantine
600 effects and its application to analysis of Covid-19 pandemia in Poland in March-April 2020.
601 *arXiv:2005.14532 [physics, q-bio]*. arXiv: 2005.14532.
- 602 Piguillem, F. and Shi, L. (2020). Optimal COVID-19 Quarantine and Testing Policies. EIEF
603 Working Papers Series 2004, Einaudi Institute for Economics and Finance (EIEF).
- 604 Robert Koch Institute (2020). Nationale teststrategie – wer wird in
605 Deutschland getestet. [cited 2020 September 23]. Available from:
606 [https://www.rki.de/DE/Content/InfAZ/N/Neuartiges_Coronavirus/Teststrategie/Nat-](https://www.rki.de/DE/Content/InfAZ/N/Neuartiges_Coronavirus/Teststrategie/Nat-Teststrat.html?nn=13490888)
607 [Teststrat.html?nn=13490888](https://www.rki.de/DE/Content/InfAZ/N/Neuartiges_Coronavirus/Teststrategie/Nat-Teststrat.html?nn=13490888).
- 608 Rong, X., Yang, L., Chu, H., and Meng, F. (2020). Effect of delay in diagnosis on transmission of
609 COVID-19. *Math. Biosci. Eng.*, 17:2725 – 2740.
- 610 Saldaña, F., Flores-Arguedas, H., Camacho-Gutiérrez, J. A., and Barradas, I. (2020). Modeling the
611 transmission dynamics and the impact of the control interventions for the COVID-19 epidemic
612 outbreak. *Math. Biosci. Eng.*, 17:4165 – 4183.

- 613 Sanche, S., Lin, Y. T., Xu, C., Romero-Severson, E., Hengartner, N., and Ke, R. (2020). High
614 contagiousness and rapid spread of severe acute respiratory syndrome coronavirus 2. *Emerging*
615 *Infectious Diseases*, 26:1470 – 1477.
- 616 Sturniolo, S., Waites, W., Colbourn, T., Manheim, D., and Panovska-Griffiths, J. (2021). Testing,
617 tracing and isolation in compartmental models. *PLoS Comput Biol*, 17:e1008633.
- 618 Surkova, E., Nikolayevskyy, V., and Drobniowski, F. (2020). False-positive COVID-19 results: Hid-
619 den problems and costs. *Lancet Respir Med*. [Advance online publication 29 Sept. 2020]. Available
620 from: [https://www.thelancet.com/journals/lanres/article/PIIS2213-2600\(20\)30453-7/fulltext](https://www.thelancet.com/journals/lanres/article/PIIS2213-2600(20)30453-7/fulltext).
- 621 Tuite, A. R., Fisman, D. N., and Greer, A. L. (2020). Mathematical modelling of COVID-19
622 transmission and mitigation strategies in the population of Ontario, Canada. *Can. Med. Assoc.*
623 *J.*, 192:E497–E505.
- 624 van den Driessche, P. and Watmough, J. (2002). Reproduction numbers and sub-threshold endemic
625 equilibria for compartmental models of disease transmission. *Mathematical Biosciences*, 180:29–
626 48.
- 627 Verma, V. R., Saini, A., Gandhi, S., Dash, U., and Koya, S. F. (2020). Capacity-need gap in hospital
628 resources for varying mitigation and containment strategies in India in the face of COVID-19
629 pandemic. *Infect. Dis. Model.*, 5:608–621.
- 630 Walsh, K. A., Jordan, K., Clyne, B., Rohde, D., Drummond, L., et al. (2020). SARS-CoV-2
631 detection, viral load and infectivity over the course of an infection. *Journal of Infection*, 81:357
632 – 371.
- 633 Widders, A., Broom, A., and Broom, J. (2020). SARS-CoV-2: The viral shedding vs infectivity
634 dilemma. *Infection, Disease and Health*, 25:210 – 215.
- 635 World Health Organization (2020a). Coronavirus disease 2019 (COVID-19): WHO
636 Thailand situation report - 19 March 2020. [cited 2020 September 23]. Avail-
637 able from: [https://www.who.int/docs/default-source/searo/thailand/2020-03-19-tha-sitrep-26-](https://www.who.int/docs/default-source/searo/thailand/2020-03-19-tha-sitrep-26-covid19.pdf?sfvrsn=6f433d5e_2)
638 [covid19.pdf?sfvrsn=6f433d5e_2](https://www.who.int/docs/default-source/searo/thailand/2020-03-19-tha-sitrep-26-covid19.pdf?sfvrsn=6f433d5e_2).

- 639 World Health Organization (2020b). Laboratory testing strategy recommendations for COVID-19.
640 [cited 2020 August 11]. Available from: <https://apps.who.int/iris/handle/10665/331509>.
- 641 Youssef, H., Alghamdi, N., Ezzat, M. A., El-Bary, A. A., and Shawky, A. M. (2021). Study on
642 the SEIQR model and applying the epidemiological rates of COVID-19 epidemic spread in Saudi
643 Arabia. *Infect. Dis. Model.*, 6:678–692.
- 644 Zaric, G. S. and Brandeau, M. L. (2001). Resource allocation for epidemic control over short time
645 horizons. *Mathematical Biosciences*, 171(1):33 – 58.